Kalahari 008, 009

Anorthositic regolith,basaltic fragmental (polymict) breccias
598, 13500 g

Figure 1: Kalahari 009 with a 1 cm scale cube (photo courtesy of A. Bischoff).

Introduction

Kalahari 008 and 009 (Fig. 1) were found in September 1999, in Botswana, in front of a sand dune in the Kalahari desert (Fig. 2). Kalahari 008 is a feldspathic regolith breccia (Fig. 3a) and Kalahari 009 is a fragmental basaltic breccia (Fig. 3b). These meteorites are very different in lithology, but are proposed to be paired due to their close find proximity, very short cosmic ray exposure ages, fayalitic olivine, and possibility that they could form in a lunar setting (Sokol and Bischoff, 2005a,b; Russell et al., 2005).

Figure 2: Region of Botswana in which Kalahari 008 and 009 were found.

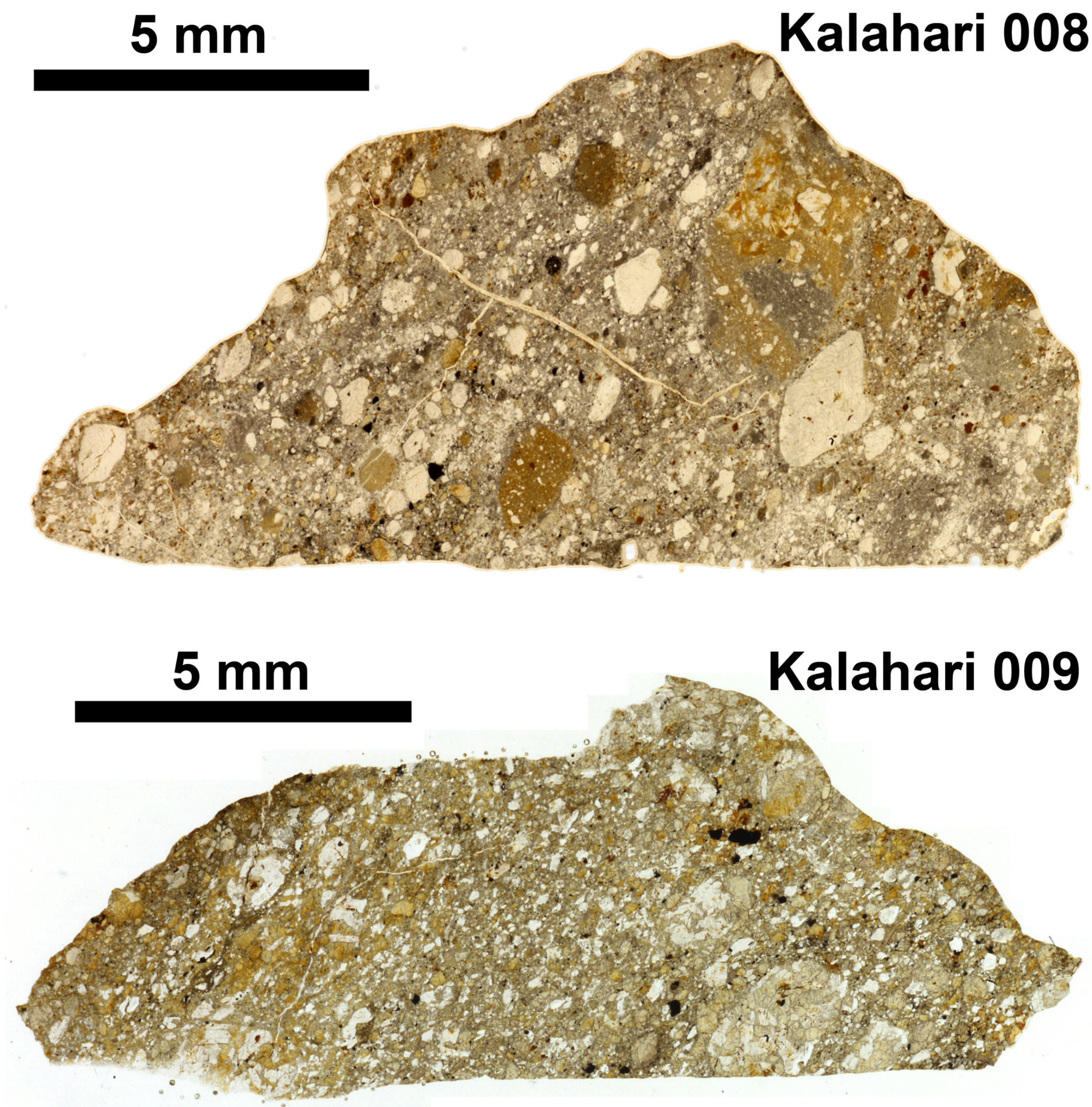

Figure 3: Plane polarized light images of thin section of Kalahari 008 (a) and 009 (b) (photos courtesy of A. Bischoff).

Petrography and mineralogy

Kalahari 008 contains feldspathic impact melt breccias, granulitic breccias, and cataclastic anorthosites (Sokol and Bischoff, 2005). This meteorite also contains solar wind implanted gases (Russell et al., 2005), and glassy spherules (Fig. 4a) consistent with a regolith origin. Plagioclase feldspars are An_{86} to An_{99} in composition (Fig. 5), and olivines are Fa_{28} to Fa_{98} (Fig. 6). The impact melt clasts are similar in composition to Apollo 16 impact melt breccias (Cohen, 2005).

Kalahari 009 is a fragmental basaltic breccia containing various basaltic clasts (Fig. 4b) in a fine grained matrix (Sokol and Bischoff, 2005b). Dominant phases in this sample are pyroxene, plagioclase, and olivine. Some of the pyroxenes have fine exsolution lamellae. Minor and accessory phases include ilmenite, chromite, troilite, ulvospinel, and FeNi metal. A common occurrence of silica-hedenbergite-fayalite intergrowths is attributed to the breakdown of pyroxferrite (Fig. 4c; Sokol and Bischoff, 2005b). Plagioclase feldspars are largely An_{88} to An_{96} in composition (Fig. 5), and olivines are Fa_{52} to Fa_{99} (Fig. 6). Pyroxenes in clasts and fragments very in composition

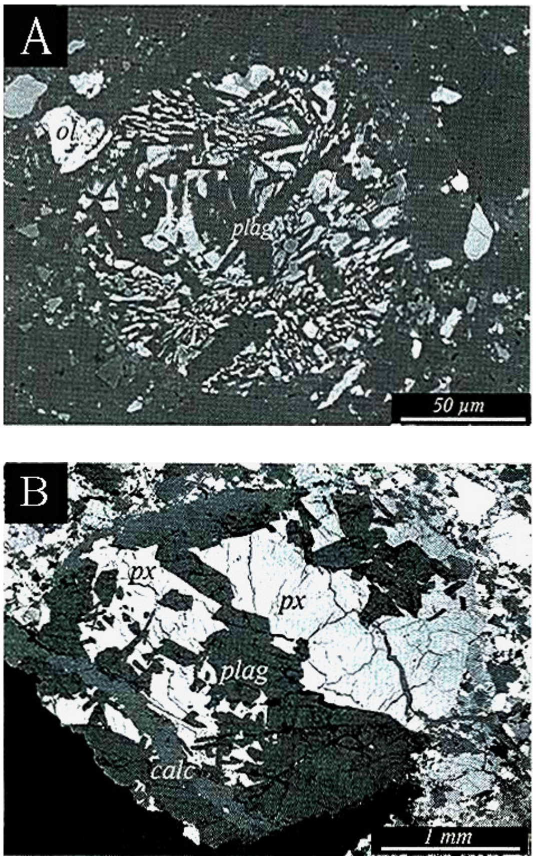

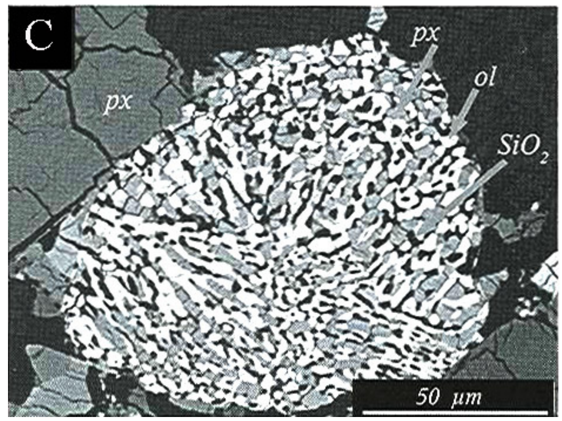

Figure 4: Back scattered electron images of clasts from Kalahari 008 and 009. Figure 4a: Devitrified spherule in Kalahari 008. Figure 4b: typical subophitic basalt textured clast in Kalahari 009. Figure 4c: symplectite of silica (black,) hedenbergite (grey) and fayalite (white) in Kalahari 009. All images from Sokol and Bischoff (2005).

out to ferro-augites, similar to pyroxenes in Apollo 12 and 15 rocks (Fig. 7; Papike et al., 1976). There are no solar wind gases detected in this meteorite, as opposed to Kalahari 008 (Russell et al., 2005).

Chemistry

The bulk composition of Kalahari 008 is typical of many feldspathic lunar meteorites with 4.7% FeO and 0.75 ppm Sm (Korotev et al., 2008). Kalahari 009 has more unusual composition for a basaltic meteorite with low FeO, TiO_2, incompatible elements, and trivalent REE (Korotev et al., 2008; Schulz et al., 2007).

Radiogenic age dating

Initial age dating for Kalahari 009 was done using the ^{39}Ar-^{40}Ar approach (Fig. 8; Fernandes et al., 2006; Sokol et al., 2008). Although the lower temperature part of the spectrum appears to be disturbed, the higher temperature fractions (>0.6) indicate an age as old as 2.7 Ga, but ranging down to 1.7 Ga (Fernandes et al., 2007a, b). Dating of phosphates using U-Pb and ion microprobe analysis results in a much older age of 4.35 ± 0.10 Ga (Fig. 9; Terada et al., 2007). These older ages are supported by Rb-Sr and Sm-Nd ages of 4.30 ± 0.05 Ga (Fig. 10; Shih et al., 2008), and Lu-Hf isochron ages of ~4.2 Ga (Schulz et al., 2007) and 4.286 Ga (Sokol et al., 2008; Fig. 11). These older ages suggest that the Ar ages reflect resetting from a younger impact event (e.g., Fernandes et al., 2007b). The Sr and Nd isotopic results suggest a connection between the Kalahari 009 VLT basalt and aluminous mare basalt from Apollo 14 (Fig. 12; Shih et al., 2008). On the other hand, the very radiogenic initial $^{176}Hf/^{177}Hf$ (εHf = +12.9 ± 4.6), and low REE, Th and Ti concentrations indicate that Kalahari 009 formed from re-melting of mantle material that had undergone strong incompatible trace element depletion early in lunar history (Sokol et al., 2008). Additionally, ages of impact melt clasts in the feldspathic Kalahari 008 have been measured in two samples, yielding 2.05 and 2.08 Ga (Cohen, 2008).

Cosmogenic isotopes and exposure ages

One of the most distinctive features of this meteorite pairs is their very short exposure ages. Nishiizumi et al. (2005) measured an Earth-Moon transit time of 230 ± 90 yr. An age this young might indicate a non meteoritic age, but the ^{36}Cl content is higher than that which would be expected for in situ production from a terrestrial sample; the excess ^{36}Cl must have been produced in space (Nishiizumi et al., 2005). The combined ^{26}Al and ^{36}Cl 4π exposure ages are 350 ± 120 yr for Kalahari 008 and 220 ± 40 yr for Kalahari 009 which are the shortest exposure ages of any meteorite (Sokol et al., 2008). These ages imply that the transition time from the Moon to the Earth was 230 ± 90 yr and ejection depth was more than >1100 g/cm^2 (367 cm assuming density of 3 g/cm^3) on the Moon (Sokol et al., 2008).

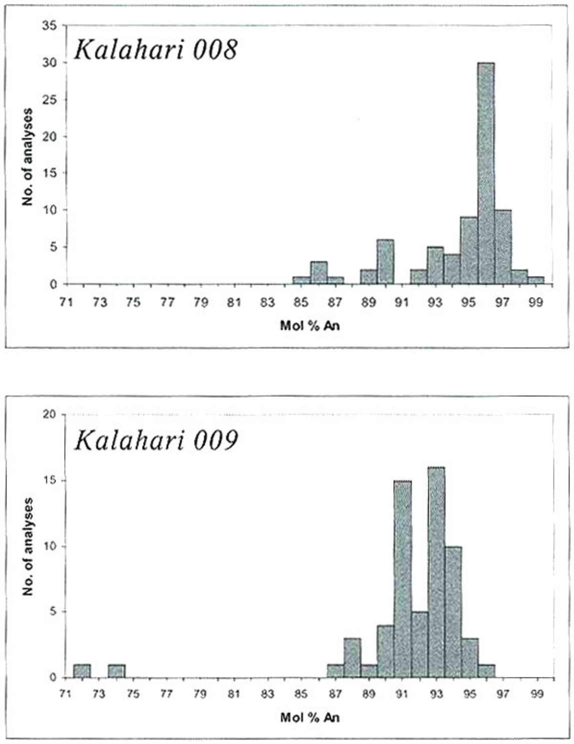

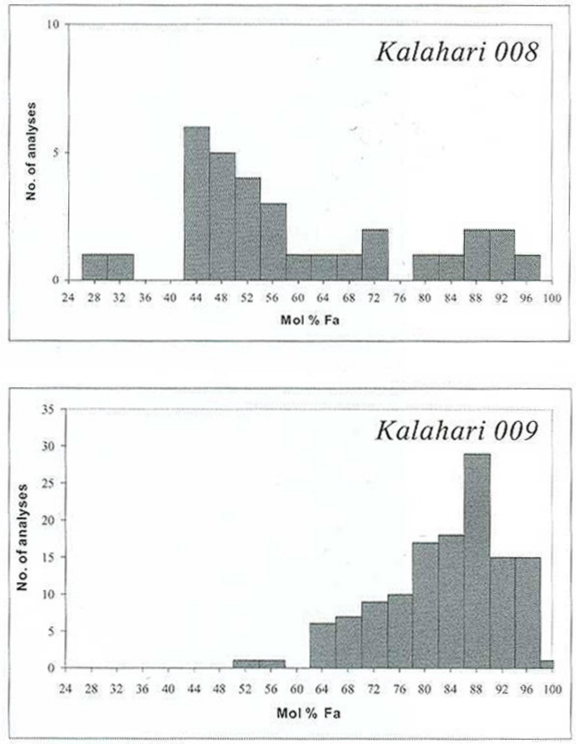

Figure 5: Plagioclase feldspar compositions in Kalahari 008 and 009 (from Sokol and Bischoff, 2005). Figure 6: Olivine compositions in Kalahari 008 and 009 (from Sokol and Bischoff, 2005).

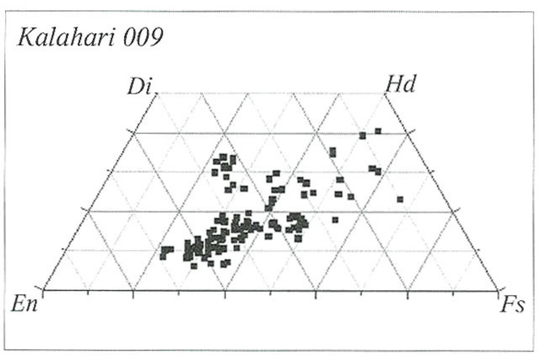

Figure 7: Pyroxene compositions from Kalahari 009 (from Sokol and Bischoff, 2005).

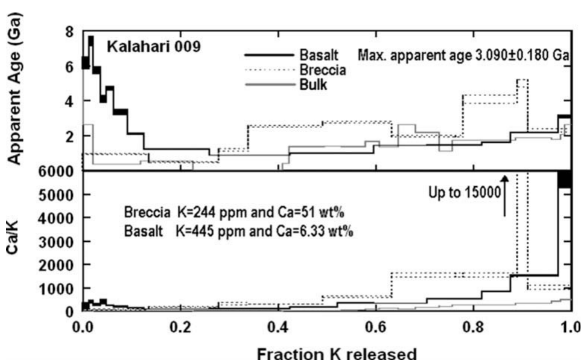

Figure 8: ^{39}Ar-^{40}Ar spectrum for Kalahari 009 (from Fernandes et al., 2006; Sokol et al., 2008). Although the lower temperature part of the spectrum appears to be disturbed, the higher temperature fractions (>0.6) indicate an age as old as 3.09 Ga.

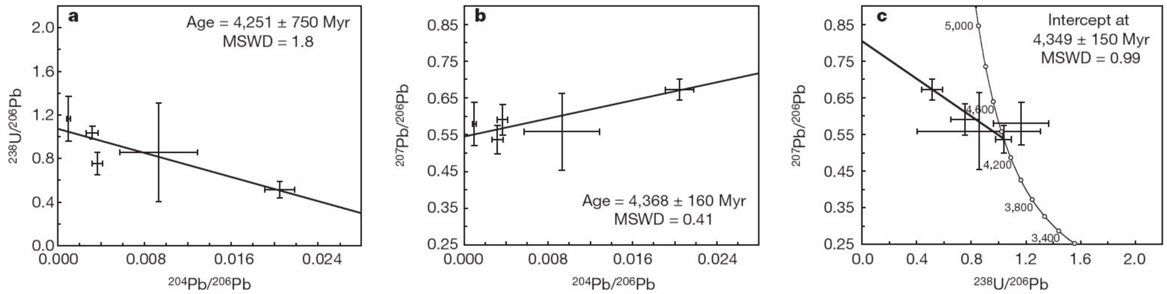

Figure 9: Results of U-Pb dating of phosphates in Kalahari 009, in an inverse U-Pb (a), inverse Pb-Pb (b) and projection in three dimensional space of the total Pb isochron (from Terada et al., 2007).

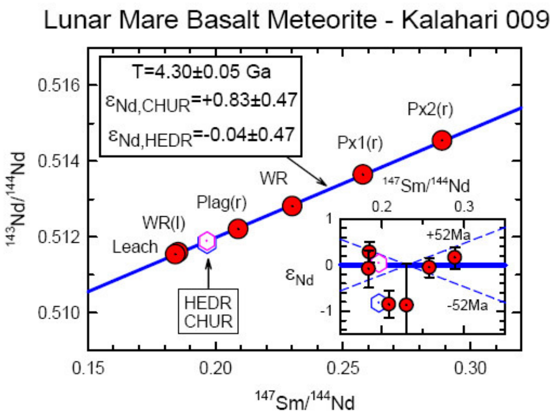

Figure 10: ^{147}Sm-^{143}Nd isochron for Kalahari 009 (from Shih et al., 2008), yielding an age of 4.30 Ga.

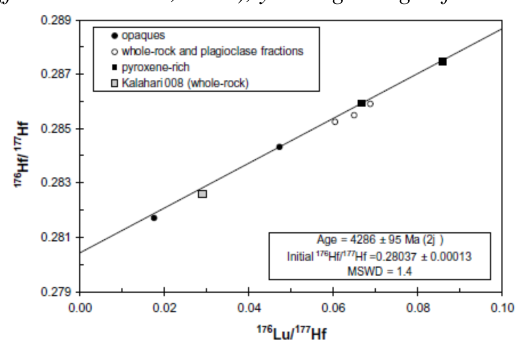

Figure 11: ^{176}Lu-^{176}Hf isochron for Kalahari 009 (from Sokol et al., 2008), yielding an age of 4.286 Ga.

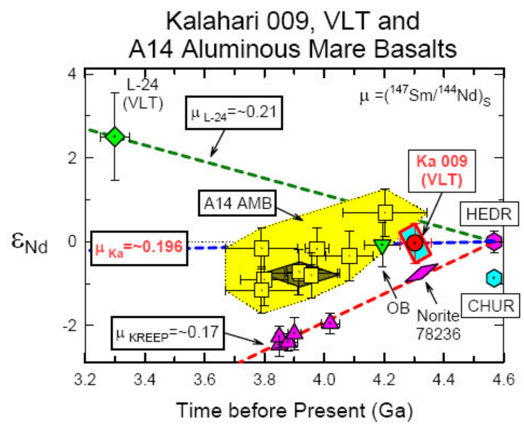

Figure 12: Epsilon Nd versus time for Kalahari 009 samples showing the nearly chondritic Sm/Nd at 4.3 Ga, similar to Apollo 14 aluminous mare basalt (from Shih et al., 2008).

Table 1a. Chemical composition of Kalahari 008 and 009

reference	1	1	2	2	2	1	1
weight	20-60	278	120	150	150	20-60	265
technique	i	e	h	e	c	i	e
	Kalahari 008	Kalahari 008	Kalahari 008	Kalahari 008	Kalahari 008	Kalahari 009	Kalahari 009
SiO_2 %	45		44.4			47.7	
TiO_2	0.51		0.28			0.26	
Al_2O_3	28.6		27.74			14.85	
FeO	4.67		5.06	4.44		16.43	
MnO	0.07		0.07	0.06		0.25	
MgO	4.62		4.44			7.95	
CaO	15.1		15.5	14.9		11.1	
Na_2O	0.58			0.54		0.5	
K_2O	0.13			0.16		0.17	
P_2O_5	0.03		0.06			0.24	
S %							
sum							
Sc ppm		10.9		10			53.2
V							
Cr		710		690			2880
Co		10.8		10.8			26.3
Ni		61		64			<150
Cu							
Zn							
Ga				2.8			
Ge							
As		0.32		0.28			<4.
Se		<0.5		0.34			<0.7
Rb		<5		3.6			<15
Sr		200		200			120
Y							
Zr		<60		34	16.78		<200
Nb					0.94		
Mo							
Ru							
Rh							
Pd ppb							
Ag ppb							
Cd ppb							
In ppb							
Sn ppb							
Sb ppb							
Te ppb							
Cs ppm		<0.1		0.063			<0.4
Ba		46		65			<90

La	1.48	1.3		0.95
Ce	3.59	4.5		2.43
Pr				
Nd	2.4	3.5		<15
Sm	0.747	0.9		0.603
Eu	1.014	0.82		0.48
Gd				
Tb	0.183	0.17		0.2
Dy		0.95		
Ho		0.24		
Er				
Tm				
Yb	0.748	0.7		1.25
Lu	0.108	0.11	0.09636	0.19
Hf	0.53	0.58	0.4699	0.4
Ta	0.07	0.07	0.0511	<0.2
W ppb				
Re ppb				
Os ppb				
Ir ppb	1.9	3.5		<9
Pt ppb				
Au ppb	1.3			<8
Th ppm	0.172	0.18		<0.2
U ppm	0.11	0.07		<0.8

technique (a) ICP-AES, (b) ICP-MS, (c) IDMS, (d) Ar, (e) INAA, (f) RNAA (g) SSMS, (h) XRF, (i) EMPA

Table 2b. Light and/or volatile elements for Kalahari 008 and 009

Li ppm		
Be		
C		
S		
F ppm		
Cl		
Br	0.49	0.8
I		
Pb ppm		
Hg ppb		
Tl		
Bi		

References: 1) Korotev et al. (2009b); 2) Sokol et al. (2008)